Friction Stir Welding and Processing VIII
Edited by: Rajiv S. Mishra, Murray W. Mahoney, Yutaka Sato, and Yuri Hovanski
TMS (The Minerals, Metals & Materials Society), 2015

Development of FSW Simulation Model-Effect of Tool Shape on Plastic Flow

Yurika Miyake[1], Fumikazu Miyasaka[1], Shuhei Matsuzawa[1], Shunta Murao[1], Kenta Mitsufuji[1], Shinnosuke Ogawa[1]

[1]Adaptive Machine Systems, Osaka University, Osaka 565-0871, Japan

Keywords: FSW, MPS method, Particle methods, Numerical analysis, Onion ring, Mesh less.

Abstract

The friction stir welding (FSW) is known as non-melting joining. Numerical analysis methods for FSW also have been developed. In these models, general grid methods have traditionally been used. However, there are some problems when these methods are employed. Calculation of the advection term for both momentum and temperature needs technical attention. To analyze a few substances of different physical properties such as the phase transformation on the bonded interface or the dissimilar joining, some complex process is required. In this study, these problems are avoided by adopting particle methods for FSW simulation. Lagrange approach is mainly used, so this particle methods calculate mass transfer and surface deformation more easily than general grid methods. The effectiveness of this method is verified by plastic flow around the tool examined by particle trace. As a result, phase transformation and tool's shape change are taken into account for the analysis of the material flow around the tool.

Introduction

The friction stir welding (FSW) is developed at the Welding Institute in 1991 [1] and has been used widely in the field of industry. Numerical analysis models for FSW also have been developed and there are many papers about it [2]-[6]. Traditionally, FDM and FEM are used for the analysis method. However, the metal around tool is deformed and stirred very intensively during FSW so that large deformation of surface of the work piece takes place. These methods using mesh or grid are difficult to handle such surface deformation. Therefore, in this paper, particle methods without mesh or grid proposed for analysis of FSW. In this method, the behavior of metal being stirred can be described directly as moving of particles. The particles can move keeping variables such as momentum, mass and enthalpy, therefore, the advection term or substance transfer can be dealt with very simply and automatically. Moreover, the mass conservation is also satisfied automatically.

This study has shown the usability of particle methods so far by performing the analysis of various FSW simulation models such as FSSW, dissimilar FSW, and general FSW. In this paper, two models which have different shapes of probe are employed. The influence of the difference in the shape of probe can be appeared by the analysis results.

Numerical model

In this paper, the plastic flow of metal during FSW is approximately described as highly viscous fluid. The governing equations for plastic flow are equations of Navier-Stokes and mass conversation. These equations are respectively given by:

$$\frac{D\boldsymbol{u}}{Dt} = -\frac{1}{\rho}\nabla P + \nu\nabla^2\boldsymbol{u} + \boldsymbol{g} \qquad (1)$$

$$\frac{D\rho}{Dt} = 0 \quad (2)$$

where ρ is density, P is pressure, ν is dynamic viscosity, $\boldsymbol{u}$ is velocity and $\boldsymbol{g}$ is gravity acceleration. The way to decide the value of ν is described later in Eq. (5). *D/Dt* denotes Lagrangian derivative which means a derivative with respect to a moving coordinate system. In this paper, Lagrangian formulation is employed to these equations so that the advection term, which is likely to be cause of numerical error, does not need to be calculated in the particle methods.

In FSW, the heat transfer is quite important factor. This thermal reaction is governed by the thermal diffusion equation as follows:

$$\frac{DT}{Dt} = \frac{k}{\rho C_p}\nabla^2 T + \frac{Q_h}{\rho C_p} \quad (3)$$

Here C_p is specific heat, k is thermal conductivity, T is temperature, and $Q_h$is heat generation per unit volume. The definition of Q_h is discussed later in Eq. (10).

The distribution of viscosity depends on temperature and equivalent strain rate. The viscosity of metal as plastic flow, which is employed in Navier-Stokes equations, is generally described as follows [10]:

$$\eta = \frac{\sigma(\dot{\varepsilon},T)}{3\dot{\varepsilon}} \quad (4)$$

$$\nu = \frac{\eta}{\rho} \quad (5)$$

where η is viscosity, $\dot{\varepsilon}$ is equivalent strain rate and σ is equivalent flow stress. Dynamic viscosity which is need for Eq. (1) is obtained by Eq. (5).

Using velocity distribution, the equivalent strain rate at each calculation point is obtained as follows:

$$\dot{\varepsilon} = \left(\frac{2}{3}\dot{\varepsilon_{\iota J}}\dot{\varepsilon_{\iota J}}\right)^{1/2} \quad (6)$$

$$\dot{\varepsilon_{\iota J}} = \frac{1}{2}\left(\frac{\partial u_i}{\partial x_j} + \frac{\partial u_j}{\partial x_i}\right) \quad (7)$$

Therefore, technically, when the value of equivalent flow stress is obtained, then the viscosity is obtained by Eq. (4), (6) and (7). Regardless of temperature and equivalent strain rate, the value of equivalent flow stress depends on material. In this paper, equivalent flow stress is approximated by equations below [9]:

$$\sigma = \frac{1}{\alpha}\ln\left\{\left(\frac{Z}{A}\right)^{\frac{1}{n}} + \left[\left(\frac{Z}{A}\right)^{\frac{2}{n}} + 1\right]^{\frac{1}{2}}\right\} \quad (8)$$

$$Z = \dot{\varepsilon}\exp\left(\frac{Q}{RT}\right) \quad (9)$$

where R is gas constant, α, A, n, Q are material constants. In this paper, A1100 is chosen for material of work piece. Material constants including α, A, n, Q for these aluminum are summarized in Table 1.

During FSW, heat is generated due to plastic deformation. In this paper, this heat generation is calculated as follows:

$$Q_h = \sigma\dot{\varepsilon} \cdot 0.9 \tag{10}$$

Eq. (10) means that 90 % of the work for plastic deformation is transformed into heat.

Table 1 Material constants for A1100

Material	A1100
Density[kg/m^3]	2710
thermal conductivity[W/m·K]	234
specific heat[J/Kg·K]	900
α[MPa^{-1}]	0.045
A	exp(24.67)
N	5.66
Q	158300

Particle methods

Particle methods are developed for hydrodynamics problem. In particle methods, the fluid moves as particles in terms of variables from Lagrangian formulation. Unlike FEM with both nodes and element, only nodes (particles) are used in particle methods so that there is no need to care about distortion of elements. Therefore, the behavior of fluid with large deformation could be analyzed without any complex operations.

There are some traditional particle methods such as MPS method [7] and SPH method [8]. In this paper, MPS method is adopted, but it is expected that SPH method or other particle methods also can get similar numerical results. In MPS method, to solve Eq. (1) and (2), the differential operators at particle i such as ∇P_i and $\nabla^2 \boldsymbol{u_i}$ are discretized by interaction among other particles j within a certain radius of r. ∇P_i and $\nabla^2 \boldsymbol{u_i}$ of are respectively expressed as follows [7]:

$$\nabla P_i = \frac{d}{W}\sum_{j\neq i}\left[\frac{P_j - P_i}{|{r_{ij}}^2|}\boldsymbol{r}_{ij} w\left(|\boldsymbol{r}_{ij}|\right)\right] \tag{11}$$

$$\nabla^2 \boldsymbol{u}_i = \frac{2d}{W}\sum_{j\neq i}\left[\frac{\boldsymbol{u}_j - \boldsymbol{u}_i}{|{r_{ij}}^2|} w\left(|\boldsymbol{r}_{ij}|\right)\right] \tag{12}$$

Here P_i and $\boldsymbol{u_i}$ are respectively pressure and velocity at particle i, $\boldsymbol{r_{ij}}$ is distance between particle i and j, and d is a number of space dimension (in this paper, d=3). Other variables are presented as follows [8]:

$$w\left(|\boldsymbol{r}_{ij}|\right) = \begin{cases} \frac{r}{|r_{ij}|} - 1 & \left(0 \le |\boldsymbol{r}_{ij}| \le r\right) \\ 0 & \left(r < |\boldsymbol{r}_{ij}|\right) \end{cases} \tag{13}$$

$$W = \sum_{j\neq i} w\left(|\boldsymbol{r}_{ij}|\right) \tag{14}$$

In MPS method, Eq. (13) is called weight function. It should be noticed that the interactions among particles are weighted averaged in Eq. (11) and (12) using Eq. (13) and (14). The shorter the distance between particles is, the stronger the interaction of the particles is. In general, the value of r is about two times the minimum distance between particles at initial placement.

Using Eq. (12), the diffusion term in Eq. (1) is usually computed explicitly. However, as we see later, the distribution of viscosity differs entirely from linear and has quite large value. In such case, it is well known that explicit calculation tends to get some errors. Therefore in this paper, the diffusion term in Eq. (1) is resolved implicitly.

Analyzed model

The illustration of analyzed model is shown in Fig. 1. The initial particle arrangement which correspond to Fig.1 is shown in Fig.2. The work piece is handled as highly viscous fluid though only edge of it is handled as rigid solid. In Fig.2, yellow particles represent the "rigid particles" and red and blue particles represent "fluid particles". The red and blue particles are the same material which colored only to ease to clear the movement of each particles. There are two models which difference is the shape of the probe. Model 1 has a cylindrical probe shown in Fig.1 (b) and Fig.2 (a). Model 2 has a truncated conical probe shown in Fig.1 (c) and Fig. 2 (b). In both models, the tool has an angle of three degrees. The actual shape of the probe has little taper and probe has thread in usual experiment. In this paper, however, the vertical velocity which corresponds to the effect of thread is added on the lateral face particles of probe. This additional velocity is presented as follows:

$$u_z = \Delta L \times n_s \tag{15}$$

where u_z is additional velocity, ΔL is the pitch of thread, n_s is rotating speed.

The process of FSW includes three phase. First phase is plunging process in which the tool is plunged into work piece until the bottom of shoulder is in contact with surface of work piece. The second phase is dwelling process in which the tool keeps only rotating in a few seconds. In this process the temperature develop enough to sir the work piece. The third phase is welding process in which the tool starts to go on the joint line and after a while the plastic flow and temperature field becomes quasi-stationary state.

In this paper, however, only the welding process is reported. In this calculation, besides, the initial temperature of whole model is equal to room temperature and the initial velocity field is zero.

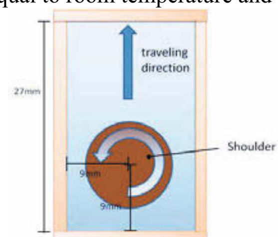

Fig.1 (a) Plane view of analyzed model

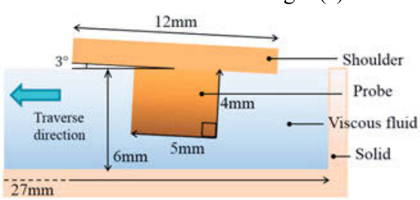

Fig.1 (b) Front view of analyzed Model 1

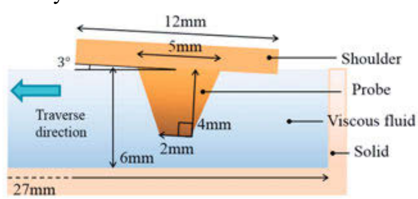

Fig.1 (c) Front view of analyzed Model 2

Fig. 1 Illustration of analyzed Model

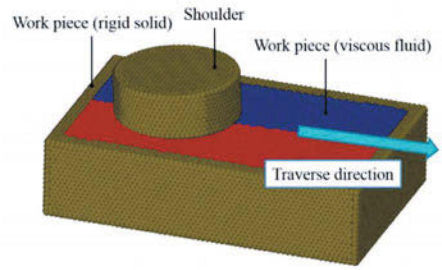

Fig.2 (a) Whole particles in model


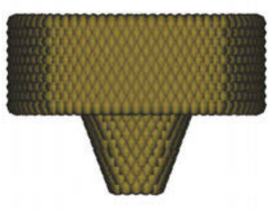

Fig.2 (b) Tool particles in Model 1 Fig.2 (c) Tool particles in Model 2

Fig. 2 Initial particle arrangement in the calculation

Analyzed results

Using two different models in Fig. 1 (b) and Fig. 1 (c), the influence of the shape of the probe on the material flow around the tool can be investigated. In this calculation, A1100 is employed as the material of the work piece.

In Fig. 4, the velocity field of two models is shown at 0.82 seconds on the cross section same as the view of Fig. 3. The velocity field is intensely turbulent in Fig. 4 (a) about Model 1. The turbulent flow does not appear in Fig. 4 (b) about Model 2. Furthermore, circulating flow appears in Fig. 4 (a). Fig. 5 (a) indicates the magnified view around circulating flow of Fig. 4 (a). Fig. 5 (b) indicates the magnified view of Fig. 4 (b) which is the same location of Fig. 5 (a). The figures about Model 1 show that the flow rate is so increased below the shoulder that some materials cannot move into the horizontal direction and downward material flow is generated. The radius of the truncated conical probe is smaller than that of the cylindrical probe unless below the shoulder, therefore there is not enough flowable space to make downward flow.

The temperature distributions are respectively shown in Fig. 6 at the same time in Fig. 4. Below the shoulder, the distributions look almost same. However, the distributions around the tip of probe are different. The temperature in Fig. 6 (b) is lower than that in Fig. 6 (a).

With respect to the velocity field and temperature distribution, the analyzed result is qualitatively correct to the following theory. The velocity increases in proportion to the radius by the definition of angular velocity as follows:

$$u = r\omega \tag{16}$$

The velocity influences the equivalent strain rate, equivalent flow stress and temperature increases as seen from Eq. (3) to Eq. (10).

Table 2 Condition of analysis for FSW of A1100

	Model 1	Model 2
Number of particles	70759	70746
Initial minimum particle distance[mm]	5.0e-4	
Time interval[sec]	1.0e-4	
Density of tool [kg/m^3]	2710	
Specific heat of tool [J/Kg・K]	460	
Thermal conductivity of tool[W/m・K]	24	
Traverse speed of tool [mm/min]	500	
Rotation speed of tool [rpm]	500	
Tilt angle of tool [degree]	3	
Pitch of tread on probe [mm]	0.7	
heat-transfer coefficient of air [Wm^{-2}K^{-1}]	50	
Room temperature [K]	293	

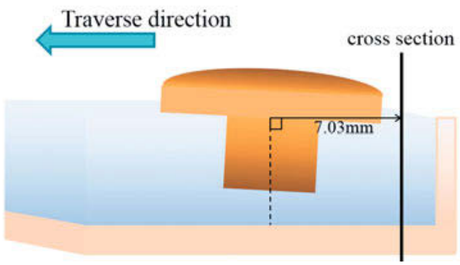

Fig. 3 Position of cross section at 0.82 seconds

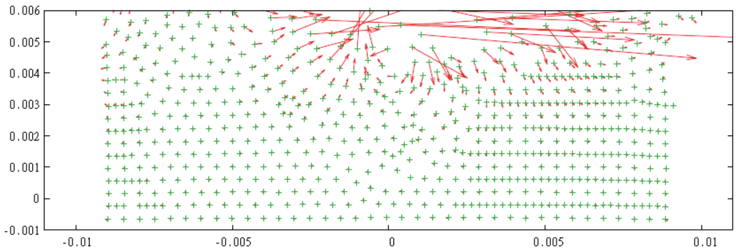

Fig. 4 (a) Model 1

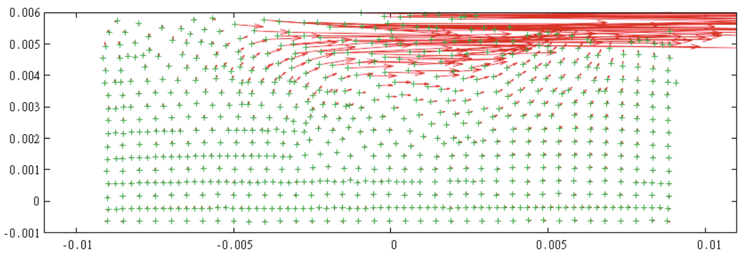

Fig. 4 (b) Model 2

Fig. 4 The velocity field at 8.02 seconds on the cross section in Fig. 3

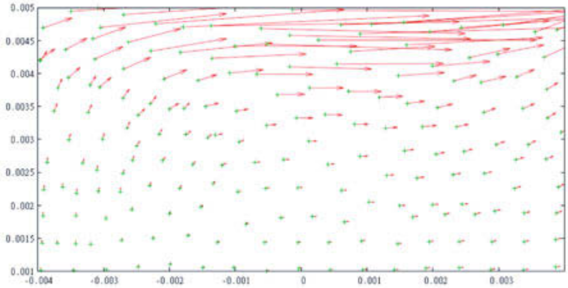

Fig. 5 (a) Model 1

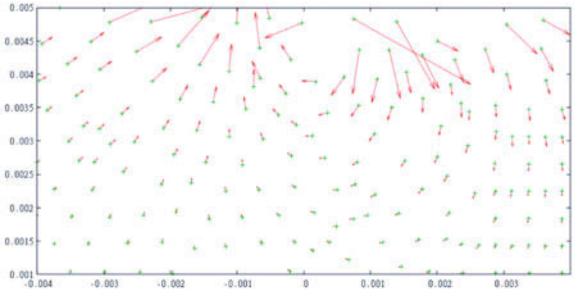

Fig. 5 (b) Model 2

Fig. 5 The magnified views of the velocity field in Fig. 4

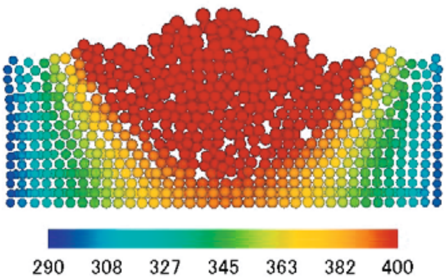

Fig. 6 (a) Model 1

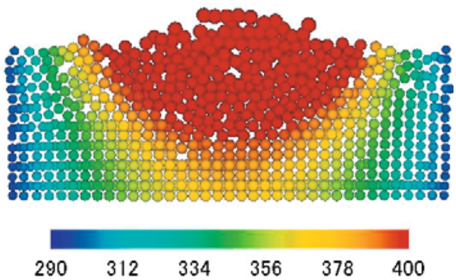

Fig. 6 (b) Model 2

Fig. 6 Temperature distributions at 0.82 seconds on the cross section in Fig. 3 [K]

Conclusions and future subjects

In this paper, the influence of the shape of the probe on the material flow around the tool is investigated. From the analyzed results about the model of the cylindrical probe, it is shown that the velocity field is turbulent and the heat widely spreads. However, the velocity field by truncated conical probe is not turbulent and the temperature of the tip of the probe is lower than that by cylindrical probe. Moreover, the circulating flow appears in the velocity field by cylindrical probe. This indicates the onion ring, which is formed behind the tool, is affected by the tool shape.

In this paper, the work piece is represented as highly viscous fluid. The phase transformation is not taken into account in this model. Therefore, this model cannot handle the defects such as tunneling defects. In future, the material of the work piece should be represented by highly viscous liquid and viscous elastomer to consider the phase transformation.

References

[1]: Thomas, M. W., Nicholas, J., Needham, J. C., Murch, M. G., Templesmith, P. and Dawes, C. J. “Friction stir butt welding.”, GB Pat. Application 9125978.8, December 1991; US Pat. 5460317, October 1995.

[2]: P. Ulysse, “Three-dimensional modeling of the friction stir-welding process”, *International Journal of Machine Tools & Manufacture* 42 (2002) 1549–1557.

[3]: S Guerdoux and L Fourment, “A 3D numerical simulation of different phases of friction stir welding”, Modelling Simul. Mater. Sci. Eng. 17 (2009) 075001 (32pp).

[4]: M Song and R Kovacevic, “Numerical and experimental study of the heat transfer process in friction stir welding”, *Proceedings of the Institution of Mechanical Engineers*, Part B: Journal of Engineering Manufacture 217 (1), pp. 73-85.

[5]: Hosein Atharifar, Dechao Lin, and Radovan Kovacevic, “Numerical and Experimental Investigations on the Loads Carried by the Tool During Friction Stir Welding”, *Journal of Materials Engineering and Performance*., 18 (4), 2009, p 339–350.

[6]: H Schmidt and J Hattel, “A local model for the thermomechanical conditions in friction stir welding”, *Modelling Simul. Mater. Sci. Eng*. 13 (2005) 77–93.

[7]:S. Koshizuka, Y. Oka, “Moving-Particle Semi-implicit Method for Fragmentation of Incompressible Fluid” *Nucl. Sci. Eng. Soc.*, vol. 123, pp. 421-434, 1995.

[8]: Gingold,R.A.& Monaghan, J. J. ,” Smoothed particle hydrodynamics – theory and application to non-spherical stars” *Mon. Not. R. astr. Soc*. 181, (1977), 375-389.

[9]: T. Sheppard and A. Jackson, “Constitutive Equations for Use in Prediction of Flow Stress During Extrusion of Aluminum Alloys”, *Mater. Sci. Tech*., 1979, 13 (3), p 203–209.

[10]: O.C. Zienkiewicz, P.C. Jain, and E. Onate, “Flow of Solids During Forming and Extrusion: Some Aspects of Numerical Solutions”, *Int. J. Solid Struct*., 1978, 14, p 15–38.